NIH Public Access
Author Manuscript
Regul Pept. Author manuscript; available in PMC 2008 December 4.

Published in final edited form as:
Regul Pept. 2007 December 4; 144(1-3): 91–100. doi:10.1016/j.regpep.2007.06.008.

Vasoactive intestinal peptide (VIP) and pituitary adenylate cyclase activating peptide (PACAP) receptor specific peptide analogues for PET imaging of breast cancer: Invitro/invivo evaluation

Kaijun Zhang, MD, PhD,
Postdoctoral fellow, Laboratory of Radiopharmaceuticals and Molecular Imaging, Department of Radiology, Thomas Jefferson University, 1020 Locust Street, Suite 361 JAH, Philadelphia, PA. 19107, USA.

Mohan R. Aruva, PhD,
Research Associate, Laboratory of Radiopharmaceuticals and Molecular Imaging, Department of Radiology, Thomas Jefferson University, 1020 Locust Street, Suite 361 JAH, Philadelphia, PA. 19107, USA.

Nylla Shanthly, MBBS, DRM,
Research Associate, Laboratory of Radiopharmaceuticals and Molecular Imaging, Department of Radiology, Thomas Jefferson University, 1020 Locust Street, Suite 361 JAH, Philadelphia, PA. 19107. USA.

Christopher A. Cardi, MS,
Research Associate, Jefferson Molecular and Biomedical Imaging Facility, Department of Radiology, Thomas Jefferson University, 233 S. 10th Street, 10 Bluemle Life Sciences Building, Philadelphia, PA. 19107. USA

Chirag A. Patel, MD, MS,
Post Doctoral Fellow, Department of Medicine, Division of Gastroenterology and Hepatology, Thomas Jefferson University, 1025 Walnut Street, Room 903 College. Philadelphia, PA 19107. USA.

Satish Rattan, DVM,
Professor, Department of Medicine, Division of Gastroenterology and Hepatology, Thomas Jefferson University, 1025 Walnut Street, Room 901 College, Philadelphia, PA 19107. USA.

Gregory Cefarone, BS,
Graduate Student, Biochemistry and Molecular Biology, Thomas Jefferson University, 233 S. 10th Street, 219 Bluemle Life Sciences Building, Philadelphia, PA. 19107. USA.

Eric Wickstrom, PhD, and
Professor of Biochemistry and Molecular Pharmacology, Kimmel Cancer Center, Thomas Jefferson University, 233 S. 10th Street, 219 Bluemle Life Sciences Building, Philadelphia, PA. 19107-5541. USA.

Mathew L. Thakur, PhD

Author for correspondence: Dr. Mathew L. Thakur Ph.D., Director, Laboratories of Radiopharmaceutical Research and Molecular Imaging, Department of Radiology, Thomas Jefferson University, Kimmel Cancer Center, 1020 Locust Street, Suite 359 JAH, Philadelphia, PA. 19107, USA. Email: Mathew.Thakur@jefferson.edu, Tel: 215-503-7874, Fax: 215-923-9245.

Publisher's Disclaimer: This is a PDF file of an unedited manuscript that has been accepted for publication. As a service to our customers we are providing this early version of the manuscript. The manuscript will undergo copyediting, typesetting, and review of the resulting proof before it is published in its final citable form. Please note that during the production process errors may be discovered which could affect the content, and all legal disclaimers that apply to the journal pertain.

NIH-PA Author Manuscript
NIH-PA Author Manuscript
NIH-PA Author Manuscript

NIH-PA Author Manuscript

NIH-PA Author Manuscript

NIH-PA Author Manuscript

Director, Laboratories of Radiopharmaceutical Research and Molecular Imaging, Department of Radiology, Thomas Jefferson University, 1020 Locust Street, Suite 359 JAH, Philadelphia, PA. 19107. USA.

Introduction

Vasoactive intestinal peptide (VIP) and pituitary adenylate cyclase-activating peptide (PACAP) receptors known as VPAC1, VPAC2 and PAC1 have been shown to be overexpressed on human tumors [1–7]. For these receptors, two primary peptides have high affinity [8,9]. First, the VIP, a 28-amino acid, hydrophobic peptide, isolated from porcine intestine [10]. VIP has three Lysine (Lys) residues (at positions 15, 20, and 21), two tyrosine (Tyr) residues (at positions 10 and 22), two Arginine (Arg) residues (at positions 12 and 14), an essential histidine (His) residue at the N terminus and (Asn) amidated C- terminus. All 28 amino acids are required for full biologic activity of VIP [11]. Second, the Pituitary Adenylate Cyclase Activating Polypeptide (PACAP). This 38-amino acid peptide is isolated from bovine hypothalamus [12]. PACAP was found to stimulate accumulation of intracellular and extracellular cAMP in rat anterior pituitary cells [13]. Later Gottschall et al [13] isolated a 27 amino acid peptide ($PACAP_{27}$) from bovine hypothalamus which they observed to have similar properties as $PACAP_{38}$. $PACAP_{27}$ shares a homology of 19 amino acids with VIP_{28}. Like VIP_{28}, $PACAP_{27}$ also has an amidated (Leu) C-terminal and His at the N-terminal.

The biological actions of VIP and PACAP are mediated by a family of three G protein-coupled receptors, which are designated as VPAC1, VPAC2 and PAC1 [14–17]. These gene receptors are also detected on the cell membrane of normal intestinal and bronchial epithelial cells [5, 7], albeit receptor density has not been specified. For human tumors on the other hand, studies have revealed that VPAC1, VPAC2, and PAC1 receptors are located at the plasma membrane of the tumor cells [18]. Among the tumors on which VPAC1 receptors have been found in high density and high incidence, include cancers of breast, prostate and urinary bladder (100%), colon (96%), pancreas (65%), lung (58%), stomach (54%), and liver (49%) [1–3].

With the goal that radiolabeled VIP_{28} can specifically target these receptors for invivo visualization of some of these human tumors, Virgolini et al labeled VIP_{28} with Iodine-123 (^{123}I) ($t_{½}$ 13.3 hr, γ=159 keV, 90%) at tyrosine position 10 and 22 [19]. Taking into consideration, the ubiquitous availability, and its predominant world wide role in nuclear medicine, we labeled VIP_{28} and $PACAP_{27}$ with ^{99m}Technetium (^{99m}Tc, t½ 6 hr, γ= 140 keV, 94%) which required modification of the peptide to covalently accommodate a group of additional amino acids to chelate ^{99m}Tc [20–22]. The use of ^{99m}Tc analogues allowed efficient imaging of human breast cancer [23–24].

Positron Emission Tomography (PET) permits high imaging resolution leading to the visualization of small tumors (2 mm). PET imaging of tumors with ^{18}Flourine (^{18}F) labeled VIP has not been highly appealing [25]. For PET imaging, our goal was to label VIP and PACAP analogues with another radionuclide, namely ^{64}Copper (^{64}Cu). This radionuclide has a longer half life ($t_{½}$ 12.7 hr, β^+= 655 keV,17.4%, β^- = 573 keV, 30%), is available commercially, has abundantly known chemistry and provides nearly quantitative yields so that labeled compound once prepared, can be injected without further purification.

In an attempt to develop VIP_{28} analogue with higher receptor affinity and better invivo stability, Bolin et al [26,27] have synthesized and characterized several analogues of VIP_{28} molecules. Based upon these data we chose two best additional VIP_{28} analogues, making a total of four. To enable labeling with ^{64}Cu, each of the four peptides was further derivatized as described in the material and method section.

NIH-PA Author Manuscript

NIH-PA Author Manuscript

NIH-PA Author Manuscript

The purpose of this investigation was to evaluate these analogues to ascertain that their biological activity and receptor specificity was not compromised as compared to those of the VIP_{28} and to determine their suitability for PET imaging of human breast cancers.

Materials and methods

Three analogues of the VIP peptide (TP3939, TP4200 and TP3982) and one of PACAP (TP3805) all named after their molecular weight were synthesized and labeled with ^{64}Cu or ^{99m}Tc. Their amino acid sequences are given in Table. 1. We have evaluated the analogues for functional activity and receptor affinity invitro, for blood clearance and invivo stability in athymic nude mice bearing T47D human breast cancer cells and for their affinity for human breast cancer specimens exvivo.

1. Synthesis of the peptide analogues

The analogues were synthesized so as to harbor a carboxy-terminus Lysine residue separated from VIP-asparagine by 4-aminobutyric acid as a spacer. The chelating agent used was diaminedithiol (N_2S_2). The synthesis and HPLC purification was carried out by the American Peptide Company, Sunnyvale, CA. Briefly, the peptides were synthesized on preloaded Polyethylene glycol (PEG) resin via 9-fluorenylmethyloxycabonyl (Fmoc) chemistry. The peptide chain was assembled on the resin by repetitive removal of Fmoc protecting group and coupling of the protected amino acid. The coupling agents used were 1, 3-diisopropyl carbodiimide (DIC) and N-Hydroxybenzotrazole (HOBt). Piperidine 20% in N, N-Dimethyl formamide (DMF) was used as de-Fmoc agent. The cyclic peptide was prepared separately, by converting the linear fragment through a lactam bond between the side chain of Lys21 and Asp25 made in a solution phase. The cyclic fragment was purified via preparative RP-HPLC and was assembled in the main chain peptide by DIC/HOBt coupling. The side chain protecting groups were cleaved and removed by treating the peptide resin with trifluoroacetic acid (TFA)/ thioanisole. The crude peptide was precipitated from cold ether and collected by filtration and purified via RP-HPLC using Triethylammonium phosphate (TEAP) and acetic acid buffer on waters C18 HPLC column. Linear gradient of acetonitrile was used. Pooled fractions were lyophilized. The peptide was verified by mass spectroscopic and amino acid analysis. The analogues were named according to their molecular weight.

2. a. Radiolabeling of peptide analogues with ^{64}Cu

High specific activity, no carrier added, ^{64}Cu (t½ of 12.7 h, β^+ 655 keV,17.4% and β^-573 keV, 30%) was obtained either from Washington University School of Medicine, St. Louis, MO, IsoTrace, Columbia, MO or from Nordion Inc, Kanata, Ontario, Canada.

To 20 μg of an analogue in 400 μL of 0.2 mol/L glycine buffer (pH 9) in a siliconized 5-mL glass test tube, were added 100 μg of $SnCl_2$ in 5μL 0.05 mol/L HCl (deprotecting agent) and (100–200 μCi) of ^{64}Cu in 1μL, 0.1 mol/L HCl. The mixture was vortexed and incubated at 90° C for 45 minutes [28].

2. b. Radiolabeling of peptide analogues with ^{99m}Tc

In this study ^{99m}Tc preparations were used only for cell binding assays when ^{64}Cu was not available. Ten ug of the analogue was dispensed in a 5 mL glass test tube to which were also added 40 μg $SnCl_2$ in 4 μL, 0.05 mol/L HCl, 10–20 mCi ^{99m}Tc in 200 μL, 0.9% NaCl, and 300 μL of 0.05 mol/L Na_3PO_4 at pH 12. The reaction mixture was vortexed and incubated at room temperature for 30 min. We then added 1 mL of 0.05 mol/L NaH_2PO_4 solution (pH 4.5) to neutralize the pH [28].

NIH-PA Author Manuscript

NIH-PA Author Manuscript

NIH-PA Author Manuscript

3. Quality Control

Radiochemical purity of each labeled analogue was determined using high-pressure liquid chromatography (HPLC) (Shimadzu Corporation, Kyoto, Japan.) coupled to a UV detector, NaI (Tl) radioactivity monitor, and a rate meter. The reverse phase C18 microbound column (4.6 mm × 250 mm) served as the stationary phase, and two solvents: 0.1%TriFluoroacetic acid (TFA) in H_2O and 0.1% TFA in acetonitrile as mobile phase. The gradient was such that 10% CH_3CN in aqueous 0.1% CF_3CO_2H to 100% CH_3CN in 0.1% CF_3CO_2H at a flow rate of 1 mL/min over 32 min at 22°C.

4. Functional Assay

VIP in large quantities is a vasodilator and muscle relaxant. The muscle relaxant property was used to assess the biological and functional activity of each analogue and compare them with those of the native VIP_{28}. The assay was based on the binding of VIP to specific receptors producing a concentration-dependent decrease in the resting tension of the Internal Anal Sphincter (IAS) smooth muscle. The effects of different concentrations of VIP_{28} and the 4 analogues were determined until maximum fall in the basal tension of IAS was reached.

4. a. Preparation of Smooth Muscle Strips

Two adult Wistar Rats were anesthetized and killed in accordance with the protocol approved by the Institutional Animal Care and Use Committee. The distal anal canal was dissected out and transferred quickly to oxygenated Krebs' physiologic solution of the following composition (in mmol/L): 118.07 NaCl, 4.69 KCl, 2.52 $CaCl_2$, 1.16 $MgSO_4$, 1.01 NaH_2PO4, 25 $NaHCO_3$, and 11.10 glucose. The adhering blood vessels and extraneous tissues containing the external anal sphincter were then removed by sharp dissection. The anal canal was opened and pinned flat with the mucosal side up on a dissecting tray containing oxygenated Krebs' solution. This was followed by removal of the mucosa using forceps and fine scissors and dissection of the IAS circular smooth muscle strips (approximately 2-mm wide and 1-cm long) from the lowermost part of the anal canal. Silk sutures were tied to both ends of the muscle strips for isometric tension measurements.

4. b. Measurement of Isometric Tension

The IAS muscle strips were transferred to 2-mL muscle baths with Krebs' solution bubbled continuously with a mixture of 95% O_2 and 5% CO_2 at 37° C. One end of the muscle strip was tied to the bottom of the muscle bath, and the other end was attached to an isometric force transducer (model FTO3; Grass Instruments, Quincy, MA). Isometric tension was measured using the PowerLab/8SP data acquisition system (ADInstruments Ltd., Castle Hill, NSW, Australia) and recorded using Chart 4.1.2 (ADInstruments Ltd.). Initially, 1 g of tension was applied to the muscle strips. The muscle strips were then allowed to equilibrate for about 1 h with occasional washings. During this equilibration period, strips developed steady tension. Only strips that developed steady tension and relaxed in response to electrical field stimulation were used. Both optimal length and base line of the muscle strips were determined [11,20, 21].

4. c. Drug response

The effect of different concentrations of VIP_{28} and the 4 analogues on the resting IAS tension was examined using cumulative concentration responses. After a given concentration–response curve was derived, the muscle strips were washed continuously for 45–60 min before testing for the concentration–response curve of another agent. Maximum relaxation (100%) of the smooth muscle strips was determined after completely relaxing the muscle strips with 10 mmol/L ethylenediaminetetraacetic acid (EDTA). The percentage of maximum fall in the IAS tone

NIH-PA Author Manuscript

NIH-PA Author Manuscript

NIH-PA Author Manuscript

was plotted against the log concentration of the respective analogue and the IC_{50} values were calculated as the concentration at which 50% of the relaxivity occurred.

5. Culture of human breast cancer cell line

Estrogen receptor-positive T47D breast tumor cells from American Type Culture Collection were maintained in RPMI 1640 medium with 2 mM L-glutamine adjusted to contain 10 mM HEPES, 1.0 mM sodium pyruvate, 1.5 g/L sodium bicarbonate, 4.5 g/L glucose and supplemented with 0.2 Units/ml bovine insulin, 90 % and fetal bovine serum, 10% at 37°C under 5% CO_2/95% air. The cells when confluent were detached using 0.25% trypsin-EDTA, washed and resuspended with RPMI-1640 medium at a concentration of approximately 5×10^6 cells/mL.

6. Cell binding assay

The T47D cells as grown above were seeded into 48 well sterile plates (Corning Incorporated-Life Sciences). To the cells (0.5×10^5 cells/well) in quadruplicate were then added increasing concentrations (from 0.01 nM-540 nM, 8 samples) of the labeled peptide and incubated 1 h in a humidified incubator at 37°C and 5% CO_2 with 95% air. The incubation was terminated by adding 0.5 ml of cold washing buffer made up of 1% BSA RPMI-1640 medium. After 5 minutes the cells were washed thrice using the same buffer. The supernatant from each wash was collected into marked test tubes. The cells were then solubilized with 1 M NaOH at 37 °C and collected in separate test tubes. The procedure was repeated thrice and all the solubilized cells collected. The cells and supernatant were counted for radioactivity in a gamma counter (Packard 5000 series, Meriden, CT). The counting data permitted us to calculate Bound/Free (B/F) radioactivity ratios and the number of peptide molecules in mole bound to cells. The data were then plotted as per Scatchard [29] and the Kd value calculated using the guidelines from Assay Guidance Manual, NIH Chemical Genomics Center [30]. The procedure was repeated for TP3939, TP3982, TP4200 and TP3805.

7. Autoradiography

The purpose of this study was to determine the receptor specific differential uptake on human breast cancer tissues versus the normal breast tissue. Freshly frozen randomly chosen and histologically proven human breast cancer (n= 13) and normal tissues (n= 7) were obtained from the institutional department of pathology. These were then sectioned into 10 μM, mounted on to clean glass slides and stored at −80°C. The mounted slides were allowed to reach room temperature and the condensed moisture dried. Approximately 10 μCi of the labeled analogue solution diluted in 200 μL of 50 mM of TRIS-HCl buffer (pH 7.4) containing 2%BSA, 2 mM EGT, 0.1mM Bacitracin and 5 mM $MgCl_2$ was layered on the tissue and incubated at room temperature (22°C) for 90 minutes. The slides were then washed thoroughly with cold, 0.9% NaCl solution, dried and exposed to a phosphor imaging plate. The plate was processed using Fujifilm Flourescent Image Analyzer, FLA-5000 (Image Gauge Version. 4.0). The procedure was repeated for 13 breast cancer and 7 normal breast tissues. Tissues incubated with each of the peptide analogue were analyzed and the photostimulated luminescence/mm^2 (PSL/mm^2) calculated for the tumor and the normal tissues.

8. Reverse Transcription & Real Time Polymerase Chain Reaction (RT-PCR)

The goal of RT-PCR was to ascertain that the human breast cancer and normal tissues on which autoradiography was performed, express VPAC1 receptors and that the receptor expression density was different in tumor tissues and normal tissues. The tissue architecture of the sample of the human breast cancer and the normal tissues was disrupted by the addition of Trizol (Invitrogen Life Technologies) in the presence of 2.3 mm Zirconia/Silica beads to release the RNA and then homogenized by rapid agitation using the procedure recommended by the

NIH-PA Author Manuscript

NIH-PA Author Manuscript

NIH-PA Author Manuscript

manufacturer (BioSpec products). The RNA was extracted and the total RNA was then reverse transcribed using the pre-developed TaqMan® assay reagents for one hour at 37°C. The resulting strand cDNA was diluted and used as a template for the PCR reaction with TaqMan® master mix using specific primers and probes for VPAC1. RT-PCR was performed using CFD-3200 DNA Engine Opticon System (Bio-rad Systems) and the following cycling conditions; 95°C for 15 s and 60°C for 1 min for 50 cycles. The expression levels of the VPAC1 were determined from the cycle threshold (CT) values normalized to human Glyceraldehyde-Phosphate Dehydrogenase (hu GAPDH) and standard curves used for calculation [31].

9. Blood Clearance

Blood clearance studies of the radiolabeled analogues were performed in mice. Rapid blood clearance of radioactivity may minimize the back ground and thereby enable a better view of the target tissue. The study was carried out for each of the four ^{64}Cu analogues in groups of 3 athymic nude mice per analogue. The labeled peptide (100–120 μCi) was administered through a lateral tail vein and samples of blood (approximately 50 μL each) were drawn at 1, 3, 5, 10, 15, 30, 45, 60, 90, 120, 180, 240 minutes and at 24 hr post administration. To facilitate rapid and reliable blood drawing, a small incision was made in the lower part of the tail and the other lateral vein was exposed. After each blood draw, pressure was applied to stop further bleeding. The samples were weighed and the radioactivity counted in a gamma counter (Packard 5000 series, Meriden, CT) along with a standard ^{64}Cu solution prepared at the time of injection. The percentage injected dose/gram (%ID/g) of blood was calculated and the mean ± SD for each time point were plotted as a function of time.

10. Invivo stability

The objective was to assess the invivo stability of the administered ^{64}Cu peptide by determining transchelation of the ^{64}Cu from the peptide to plasma proteins. Analysis was performed by using Sodium Dodecyl Sulphate Polyacrylamide Gel Electrophoresis (SDS-PAGE). Eighteen percent Tris-Glycine gel (Invitrogen life technologies) were used. ^{64}Cu labeled peptide (in this instance TP3939) was administered through the lateral tail vein of athymic nude mouse, and 0.5 ml blood collected in a heparinized eppendorf vial following euthanasia at 2–3 minutes. Serum was collected after centrifugation (2000 rpm for 10 minutes). Tris-Glycine SDS buffer and deionized water was added to the serum and loaded into a well. Molecular weight standard to facilitate estimation of the molecular weights of the various protein bands was loaded into another well. Further more ^{64}Cu labeled TP3939 incubated with Human Serum Albumin (HSA), $^{64}CuCl_2$ incubated with HSA were also applied. Incubation with the buffer was carried out as explained above. Finally incubated $^{64}CuCl_2$ alone was also applied. The voltage was maintained at 160V for 45 minutes. Analysis was performed simultaneously on two gels. One gel was stained with Coomassie blue, destained, cut and counted for radioactivity associated with each protein band in a gamma counter. The other gel was used for autoradiography, exposing the gel to a phosphor imaging plate for 18 hours after which it was stained with Coomassie blue, destained, cut and counted for radioactivity. The plate was processed using Fujifilm Flourescent Image Analyzer, FLA-5000 (Image Gauge Version. 4.0).

Results

1. Synthesis and characterization

The amino acid sequence of each analogue is given in Table. 1 together with their calculated and observed molecular weight and purity as determined by analytical HPLC.

NIH-PA Author Manuscript

NIH-PA Author Manuscript

NIH-PA Author Manuscript

2. Radiochemical purity

The radiochemical purity of each ^{64}Cu labeled peptide as determined by HPLC 95.43 ± 3.78 %, 96.85 ± 3.97 %, 94.6 ± 5.79 % and 97.5 ± 4.02 % for Cu-TP3939, ^{64}Cu-TP3982, ^{64}Cu-TP4200 and ^{64}Cu-TP3805 respectively. Retention times varied between 5.53 to 6.7 minutes. Fig. 1 represents a typical HPLC elution curve. The diagonal line represents percent gradient. Labeling efficiency was 97.77 ± 1.94 %, 96.72 ± 2.72, 97.91 ± 1.13, 97.37 ± 2.57 for ^{99m}Tc-TP3939, ^{99m}Tc-TP3982, ^{99m}Tc-TP4200 and ^{99m}Tc-TP3805 respectively.

3. Functional Assay Response

The IC_{50} values of the peptide analogues were 4.4×10^{-8}M for TP3939, 8.1×10^{-8}M for TP3982, 8.1×10^{-9}M for TP4200 and 5.3×10^{-8}M for TP3805 respectively. The unaltered VIP_{28} had an IC_{50} of 9.0×10^{-8}M (Table. 2, Fig. 2). These data suggest that the biological activity of each analogue as compared to that of the VIP_{28} was not compromised.

4. Cell binding assay

The dissociation constant (Kd) for each of the ^{99m}Tc labeled peptide analogue was calculated and found to be 0.33×10^{-9} M for ^{64}Cu-TP3939, 0.2×10^{-9} M for ^{64}Cu-TP3982, 0.72×10^{-9} M for ^{64}Cu-TP4200 and 3.3×10^{-9} M for ^{64}Cu-TP3805 (Table. 2, Fig. 3).

5. Autoradiography

The 13 human breast cancer tissues used were histopathologically diagnosed as, grade-3 invasive ductal carcinoma (n= 10), high grade in situ micropapillary carcinoma (n= 1), high grade in situ microinvasive carcinoma (n= 1) and intermediate grade 2 tubulolobular carcinoma (n= 1). In addition, seven were histologically designated as normal. The tumor/normal radioactivity ratios, calculated using the quantitative analysis of the phosphor imaging plates ranged from 2.17 to 10.93. The ratios for the invasive ductal carcinoma were; 3.36 –10.69 for ^{64}Cu-TP3939, 2.83 –10.93 for ^{64}Cu-TP3982, 3.97 –5.13 for ^{64}Cu-TP4200 and 2.17–9.55 for ^{64}Cu-TP3805. The ratios for the insitu microinvasive tumor were 2.6 for ^{64}Cu-TP3939, 3.77 for ^{64}Cu-TP4200 and 2.82 for ^{64}Cu-TP3805. For tubulolobular carcinoma the ratios were 2.94 for ^{64}Cu-TP3982 and 3.2 for ^{64}Cu-TP4200 (Table. 3). A typical image of an autoradiographic slide is shown in Fig. 4

6. RT-PCR

We measured the VPAC1 receptor expression in freshly frozen samples of human breast cancer and normal tissues by RT-PCR. Following a series of 22 runs (13 cancer tissues and 7 normal tissues) the difference in receptor expression in tumor tissue was found to be 5 –118 times greater than normal tissues. The histopathology correlated tumor to normal VPAC1 receptor expression ratios was as follows; 5 – 118 for grade-3 invasive ductal tumor tissues (n = 10), 6 for insitu micropapillary (n = 1), and 29.78 for high grade insitu microinvasive (n = 1), (Table. 3). Fig. 5 reveals a typical RT-PCR profile for the tumor sample and normal tissues.

7. Blood Clearance

The blood clearance was biphasic; the α-t½ was approximately 3.1 min, 3.25 min, 3.3 min, 3.3 min and β-t½ of approximately 120 min, 45 min, 150 min and 160 min for ^{64}Cu-TP3939, ^{64}Cu-TP3982, ^{64}Cu-TP4200 and ^{64}Cu-TP3805 respectively. A typical graph of the time versus % ID/g is displayed in Fig. 6.

8. Invivo stability

Polyacrylamide gel analysis indicated that at 2 min post injection approximately 86% of the radioactivity remained as ^{64}Cu labeled peptide. The remaining radioactivity was associated

NIH-PA Author Manuscript

NIH-PA Author Manuscript

NIH-PA Author Manuscript

with proteins of molecular weights of 6 kDa and above (lane 1). Similarly lane 2 in which the ^{64}Cu -TP3939 was incubated with HSA, there was negligible transchelation to protein. In these experiments only approximately 3 % of free $^{64}CuCl_2$ was bound to protein with molecular weight of >98 kDa (lane 3). Fig. 7.a represents the separation of protein as visualized following Coomassie blue staining. The molecular weight standards are also visualized. Fig. 7.b is the autoradiography of the various samples as explained in the methodology and in figure legends. Quantitative analysis of ^{64}Cu radioactivity distribution in various protein bands is given in Table. 4.

Discussion

Annually in the USA approximately 7 million breast biopsies are performed, approximately 80% of which (5.6 million) find benign pathology. The ability to noninvasively determine the benign or malignant status of suspected breast cancer mass found by mammography may minimize the number of millions of unnecessary, invasive biopsies; spare the patient from physical and psychological trauma as well as save health care dollars. Although great strides have been made for imaging breast cancer using magnetic resonance (MRI), computerized tomography (CT), ultrasound (US), and radionuclide imaging such as PET using ^{18}F-Fluorodeoxy glucose and SPECT using ^{99m}Tc Sestamibi, each modality suffers from serious limitations [32–40]. The need is compelling to investigate improved imaging probes that might target specific biomarkers and thereby contribute to a greater reliability and higher sensitivity and specificity for imaging malignant lesions and to excluding benign pathology.

Data are abundant that 100% of the breast cancer cells overexpress a gene product, cell surface receptors VPAC1 [1–3], so named because of the endogenous growth hormones VIP_{28} and $PACAP_{27}$. These peptides have high affinity for VPAC1 receptors [8,9]. VIP_{28} and $PACAP_{27}$ bind similarly to VPAC receptors. $PACAP_{27}$ has higher affinity for PAC1 receptors [41]. However it has been demonstrated that human breast cancer cells do not overexpress either VPAC2 or PAC1 receptors [3]. VPAC1 receptors are overexpressed on malignant cells before cell morphology is altered and in higher density than on the normal breast tissue cells. These receptors are internalised, phosphorylated and are not reexpressed on the cell membrane [42]. These data render VPAC1 receptors as highly useful biomarkers that may be probed for noninvasive PET imaging. The confirmation of the presence of these fingerprints on a suspected mass will ascertain malignancy and the absence of a benign pathology.

In this investigation we have chosen 4 apparently potent peptide analogues [26,27,3] which were synthesized, characterized, and derivatized for radiolabeling with ^{64}Cu to enable us to perform PET imaging. The purpose of this investigation was to determine: a) the biological characteristic of the probes was not compromised, b) their receptor specificity and receptor binding affinity were not altered, c) their invivo stability was not diminished, and d) that the probes bind to human breast tissues which express VPAC1 receptors and that this binding was preferential as compared to normal breast tissue.

Our data strongly demonstrate that these analogues are potent and functionally stable. For each analogue the radiolabeling efficiency for ^{64}Cu was greater than 92% and required no further purification before the probe could be injected for PET imaging. VIP_{28} is a muscle relaxant [15]. Using the muscle relaxivity assay on the IAS smooth muscle, the functional studies were performed which strongly indicated that the biological activity of none of the analogues was compromised. Similarly the binding assays as performed using human breast cancer cell line, T47D, corroborated the data equally affirmatively. The invitro receptor autoradiography studies showed 2.17 to 10.93 times greater quantity of ^{64}Cu-peptide analogues was bound to breast cancer tissues than to the normal breast tissue. Studies carried out after establishing good working techniques always yielded ratios of 2.17 and above. These data indicated that greater

NIH-PA Author Manuscript

NIH-PA Author Manuscript

NIH-PA Author Manuscript

number of VPAC1 receptors was expressed on malignant cells than on the normal. These data confirmed our previous observation in humans using ^{99m}Tc analogues [23,24] and strongly suggested that these analogues have the ability to specifically localize malignant breast lesions by PET imaging.

The data obtained using RT-PCR confirmed increased receptor expression in the tumor tissues and generally corroborated with the autoradiography data. The range of receptor expression varied from 5–118 depending on the size of the tissue and abundance of malignant cells in the sample provided.

The blood clearance data in mice for each analogue indicated rapid clearance supportive of early imaging. This clearance together with the internalization and phosphorylation of the receptors will promote diagnostic and therapeutic applications of these peptides. Certain ^{64}Cu chelates have been shown to be unstable invivo, promoting transchelation of ^{64}Cu to proteins [43]. This may hinder the invivo applications of such chelates. In our case, polyacrylamide gel analysis indicated approximately 86% of the ^{64}Cu remained bound to the peptide (4kDa) and was not transchelated to the protein invivo. Among the 15% transchelated, approximately 10% was to fraction with protein molecular weight >98 kDa (this included a significant portion that artifactually remain in the loading well, see Fig. 7, approximately 4% to protein molecular weight 50–64 kDa and 1.2 % to protein molecular weight 6–16 kDa. Approximately 50% of the ^{64}Cu clears with α t ½ of 3.0 to 3.5 minutes. Because of this rapid clearance of radioactivity, these samples were acquired 2–3 minutes post administration of the labeled analogue. Any blood drawn after 3–5 minutes post injection contains negligible radioactivity either for counting or autoradiography. To obtain some insight into the possibility of further transchelation to serum protein, we incubated the ^{64}Cu peptides with HSA invitro. These too demonstrate (Table. 4) that >97% of the activity was not transchelated to protein. This lack of transchelation is consistent with the strong chelation of ^{64}Cu to this N_2S_2 chelating moiety coupled to the peptides.

The urinary excretion of the ^{64}Cu peptide analogues for 2 hr post injection was negligible and prevented us from HPLC confirmation of enzymatic degradation of the peptide which might have eliminated in the urine. Considering together the lack of transchelation to serum proteins and the lack of urinary excretion it is reasonable to assume that the peptide remains intact. This is further evidenced by increasing quantity of radioactivity accumulating in tumors as the time elapses after its invivo administration (data not given). This stability if further witnessed by the ITLC analysis performed on urine collected from mice given ^{64}Cu -TP3982, 4 hr previously which showed that greater than 98% of activity was bound to the peptide [28]. The assumption then is that the radioactivity that binds to other normal organs, relatively large in size, may be bound to VPAC receptors expressed on the normal cells albeit at low density.

In summary all our invitro and limited invivo data strongly suggest that all of the four analogues are potent, their biological activities are not compromised and that they are worthy of further evaluation. This investigation promises to lead us to evaluate their utility for PET imaging of human breast cancers and for determining malignant lesions from benign ones.

Acknowledgements

This work was supported by NIH grant CA-109231.

We thank Dr. Juan Pallazzo MD, and Magdalena B. Potoczek of the department of Pathology for their advice and assistance in the studies of pathological specimens. Our thanks are also due to Stephanie Schulz, PhD, Department of Pharmacology and Experimental Therapeutics for the use of the homogenizer (BioSpec products).

NIH-PA Author Manuscript

NIH-PA Author Manuscript

NIH-PA Author Manuscript

References

1. Reubi JC. Neuropeptide receptors in health and disease: The molecular basis for invivo imaging. J Nucl Med 1995;36:1825–1835. [PubMed: 7562050]
2. Reubi JC. Regulatory peptide receptors as molecular targets for cancer diagnosis and therapy. Q J Nucl Med 1997;41:63–70. [PubMed: 9203845]
3. Reubi JC, Läderach U, Waser B, Gebbers JO, Robberecht P, Laissue JA. Vasoactive intestinal peptide/pituitary adenylate cyclase activating peptide receptor subtypes in human tumors and their tissues of origin. Cancer Res 2000;60:3105–3112. [PubMed: 10850463]
4. Reubi JC, Waser B, Laderach U, Srinivasan A. Pituitary adenylate cyclase activating polypeptide (PACAP) and PACAP II receptors in human tumors: invitro binding of DTPA-linked PACAP analogs [abstract]. Eur J Nucl Med 1997;24:1058.
5. Blum AM, Mathew R, Cook GA, Metwali A, Felman R, Weinstock JV. Murine mucosal T cells have VIP receptors functionally distinct from those on intestinal epithelial cells. J Neuroimmunol 1992;39:101–108. [PubMed: 1320055]
6. el Battari A, Martin JM, Luis J, Pouzol O, Secchi J, Marvaldi J, Pichon J. Solubilization of the active vasoactive intestinal peptide receptor from human colonic adenocarcinoma cells. J Biol Chem 1988;263:17685–17689. [PubMed: 2846575]
7. Couvineau A, Luburthe M. The human vasoactive intestinal peptide receptor molecule identification by covalent cross-linking in colonic epithelium. J ClinEndocrinol Metab 1985;61:50–55.
8. Zia H, Hida T, Jakowlew S, Birrer M, Gozes Y, Rheubi JC, Fridkin M, Gozes I, Moody TW. Breast cancer growth is inhibited by VIP hybrid, a synthetic VIP receptor antagonist. Cancer Res 1996;56:3486–3489. [PubMed: 8758916]
9. Zia H, Leyton J, Loecho T, Moody TW. PACAP receptors are present on breast cancer cell lines. Am Assoc Cancer Res 1997;38:117.
10. Said SI, Mutt V. Polypeptide with broad biological activity: isolation from the small intestine. Science 1970;169:1217–1218. [PubMed: 5450698]
11. Chakder S, Rattan S. The entire vasoactive intestinal polypeptide molecule is required for the activation of the vasoactive intestinal polypeptide receptor: functional and binding studies. J Pharm Exp Ther 1993;266:392–399.
12. Miyata A, Arimura A, Dahl RR, Minamino N, Uehara A, Jiang L, Culler MD, Coy DH. Isolation of a novel 38 residue-hypothalamic polypeptide which stimulates adenylate cyclase in pituitary cells. Biochem Biophys Res Commun 1989;164:567–574. [PubMed: 2803320]
13. Gottschall PE, Tatsuno I, Miyata A, Arimura A. Characterization and distribution of binding sites for the hypothalamic peptide, pituitary adenylate cyclase-activating polypeptide. Endocrinology 1990;127:272–277. [PubMed: 2361473]
14. Laburthe M, Couvineau A. Molecular pharmacology and structure of VPAC receptors for VIP and PACAP. Regul pept 2002;108:165–173. [PubMed: 12220741]
15. Laburthe M, Couvineau A, Marie JC. VPAC receptors for VIP and PACAP. Receptors Channels 2002;8:137–153. [PubMed: 12529932]
16. Le SV, Yamaguchi DJ, McArdle CA, Tachiki K, Pisegna JR, Germano PM. PAC1 and PACAP expression, signaling, and effect on the growth of HCT8, human colonic tumor cells. Regul pept 2002;109:115–125. [PubMed: 12409223]
17. Germano PM, Le SV, Oh DS, Fan R, Lieu S, Siu A, Pisegna JR. Differential coupling of PAC1 SV1 splice variant of human colonic tumors to the activation of intracellular cAMP But not intracellular Ca_2^+ does not activate tumor proliferation. J Mol Neurosci 2004;22:83–92. [PubMed: 14742913]
18. Schulz S, Rocken C, Mawrin C, Weise W, Hollt V, Schulz S. Immunocytochemical identification of VPAC1, VPAC2 and PAC1 receptors in normal and neoplastic human tissues with subtype specific antibodies. Clin Cancer Res 2004;10:8234–8242.
19. Virgolini I, Raderer M, Kurtaran A, Angelberger P, Banyai S, Yang Q, Li S, Banyai M, Pidlich J, Niederle B, Scheithauer W, Valent P. Vasoactive intestinal peptide-receptor imaging for the localization of intestinal adenocarcinomas and endocrine tumors. N Engl J Med 1994;331:1116–1121. [PubMed: 7935635]

NIH-PA Author Manuscript

NIH-PA Author Manuscript

NIH-PA Author Manuscript

20. Pallela VR, Thakur ML, Chakder S, Rattan S. Tc-99m labeled vasoactive intestinal peptide receptor agonist: functional studies. J Nucl Med Biol 1999;40:352–360.
21. Thakur ML, Aruva M, Bolewska-Pedyczak E, Gariepy J. Preparation of Cu-64 and Tc-99m-N2S2-vasoactive intestinal peptide (VIP) for imaging gene expression [abstract]. J Labelled Compds Radiopharm 2003;46:S128.
22. Chen X, Edwards WB, Anderson CJ, McCarthy TJ, Welch MJ. Solid phase synthesis of teta conjugated vasoactive intestinal peptide and invivo behavior of copper-64 radiolabeled VIP conjugate. J Labelled Compds Radiopharm 2001;44:S688.
23. Thakur ML, Marcus CS, Saeed S, Pallela V, Minami C, Diggles L, Le Pham H, Ahdoot R, Kalinowski EA. 99mTc-Labeled vasoactive intestinal peptide analog for rapid localization of tumors in humans. J Nucl Med 2000;41:107–110. [PubMed: 10647612]
24. Thakur, ML.; Marcus, CS.; Saeed, S.; Pallela, V.; Minami, C.; Diggles, L.; Pham, HL.; Ahdoot, R.; Kalinowski, EA.; Moody, T. Imaging tumors in humans withTc-99m-VIP. VIP, PACAP, Glucagon, and Related Peptides. In: Fahrsenkrug, J.; Said, SI., editors. Annals of the NY Academy of Science. 921. New York, NY: New York Academy of Science; 2000. p. 37-44.
25. Jagada EM, Aloj L, Seidel J, Lang L, Moody TW, Green S, Caraco C, Daube-Witherspoon M, Green MV, Eckelman WC. Comparison of an 18F labeled derivative of vasointestinal peptide and 2-deoxy-2-[18F] flouro-D-glucose in nude mice bearing breast cancer xenografts. Mol Imaging Biol 2002;4:369–379. [PubMed: 14537113]
26. Bolin DR, Cottrell J, Garippa R, Michalewsky J, Rinaldi N, Simko B, O'Donnell M. Structure-activity studies on the vasoactive intestinal peptide pharmacophore. 1. Analogs of tyrosine. Int J Pept Protein Res 1995;46:279–289. [PubMed: 8537181]
27. Bolin DR, Cottrell J, Garippa R, Rinaldi N, Senda R, Simko B, O'Donnell M. Comparison of cyclic and linear analogs of vasoactive intestinal peptide. Drug Des Discov 1996;13:107–114. [PubMed: 8874048]
28. Thakur ML, Aruva MR, Gariepy J, Acton P, Rattan S, Prasad S, Wickstrom E, Alavi A. PET Imaging of Oncogene Overexpression Using 64Cu-Vasoactive Intestinal Peptide (VIP) Analog: Comparison with 99mTc-VIP Analog. J Nucl Med 2004;45:1381–1389. [PubMed: 15299065]
29. http://www.graphpad.com/curvefit/scatchard_plots.htm
30. NIH Chemical Genomics Center, Assay Guidance Manual [Version 4:1; Receptor Binding Assays.htm]. http://www.ncgc.nih.gov/guidance/section5.html#saturation-binding
31. Kawakami M, Kimura T, Kishimoto Y, Tatekawa T, Baba Y, Nishizaki T, Matsuzaki N, Taniguchi Y, Yoshihara S, Ikegame K, Shirakata T, Nishida S, Masuda T, Hosen N, Tsuboi A, Oji Y, Oka Y, Ogawa H, Sonoda Y, Sugiyama H, Kawase I, Soma T. Preferential expression of the vasoactive intestinal peptide (VIP) receptor VPAC1 in human cord blood-derived $CD34^{+}CD38^{-}$ cells: possible role of VIP as a growth-promoting factor for hematopoietic stem/progenitor cells. Leukemia 2004;18:912–921. [PubMed: 14999295]
32. Yang WT, Tse GM. Sonographic, mammographic, and histopathologic correlation of symptomatic ductal carcinoma in situ. AJR Am J Roentgenol 2004;182:101–110. [PubMed: 14684521]
33. Uematsu T, Sano M, Homma K. False-positive helical CT findings of multifocal and multicentric breast cancer: is attenuation of tumor useful for diagnosing enhanced lesions? Breast Cancer 2002;9:62–68. [PubMed: 12196724]
34. Schnall M, Orel S. Breast MR imaging in the diagnostic setting. Magn Reson Imaging Clin N Am 2006;14:329–337. [PubMed: 17098174]
35. Ghai S, Muradali D, Bukhanov K, Kulkarni S. Nonenhancing breast malignancies on MRI: sonographic and pathologic correlation. AJR Am J Roentgenol 2005;185:481–487. [PubMed: 16037524]
36. Smith AP, Hall PA, Marcello DM. Emerging technologies in breast cancer detection. Radiol Manage 2004;26:16–24. [PubMed: 15377106]
37. Elmore JG, Armstrong K, Lehman CD, Fletcher SW. Screening for breast cancer. JAMA 2005;293:1245–1256. [PubMed: 15755947]
38. Berg WA, Gutierrez L, NessaIiver MS, Carter WB, Bhargayan M, Lewis RS, Ioffe OB. Diagnostic accuracy of mammography, clinical examination, US, and MR imaging in preoperative assessment of breast cancer. Radiology 2004;233:830–849. [PubMed: 15486214]

NIH-PA Author Manuscript

NIH-PA Author Manuscript

NIH-PA Author Manuscript

39. Chagpar AP, Middleton LP, Sahin AA, Dempsey P, Buzdar AU, Mirza AN, Ames FG, Babiera GV, Feig BW, Hunt KK, Kuerer HM, Meric-Bernstam F, Ross MI, Singletary SE. Accuracy of physical examination, ultrasonography, and mammography in predicting residual pathologic tumor size in patients treated with neoadjuvant chemotherapy. Ann Surg 2006;243:257–264. [PubMed: 16432360]

40. Bombardiere E, Crippa F, Baio SM, Peeters BA, Greco M, Pauwels EK. Nuclear Medicine advances in breast cancer imaging. Tumori 2003;87:277–287.

41. Garcia-Fernandez MO, Collado B, Bodega G, Cortes J, Ruiz-Villaespesa A, Carmena MJ, Prieto JC. Pituitary adenylate cyclase-activating peptide/vasoactive intestinal peptide receptors in human normal mammary gland and breast cancer tissue. Gynecol Endocrinol 2005;20:327–333. [PubMed: 16019382]

42. Langlet C, Langer I, Vertongen P, Gaspard N, Vanderwinden JM, Robberecht P. Contribution of the carboxyl terminus of the VPAC1 receptor to agonist-induced receptor phosphorylation, internalization, and recycling. J Biol Chem 2005;29:28034–28043. [PubMed: 15932876]

43. Bass LA, Wang M, Welch MJ, Anderson CJ. In vivo transchelation of copper-64 from TETA-octreotide to superoxide dismutase in rat liver. Bioconjug Chem 2000;11:527–532. [PubMed: 10898574]

NIH-PA Author Manuscript

NIH-PA Author Manuscript

NIH-PA Author Manuscript

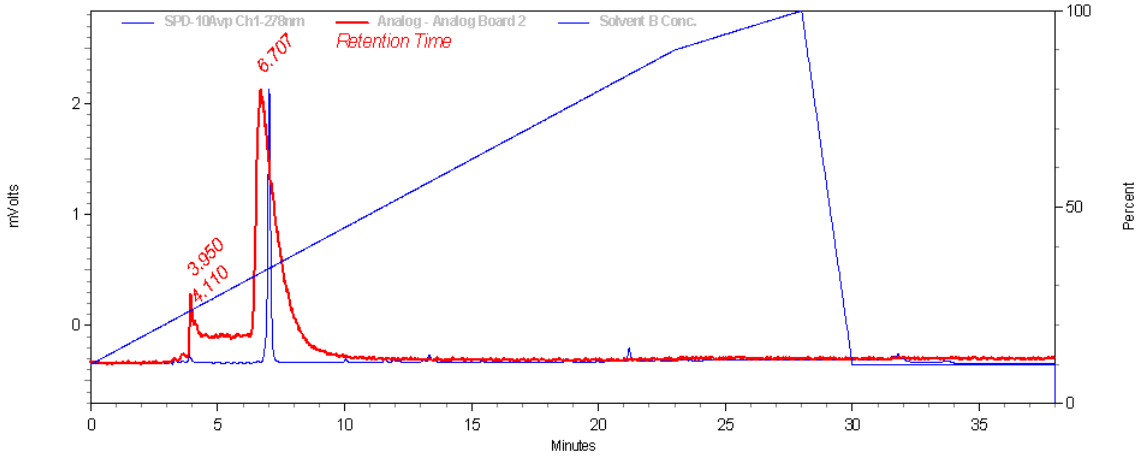

Pk #	Time	Height	Area	Area Percent
1	3.950	477	3357	3.170
2	4.110	94	339	0.320
3	6.707	2200	102219	96.510
Totals		2771	105915	100.000

Fig. 1.

HPLC elution profile of one of ^{64}Cu - TP3939, revealing 96.5% of the radioactivity is bound to a peak at 6.7 min. The UV peak is also centered around 6.7 min. The diagonal line represents % gradient as a function of time.

NIH-PA Author Manuscript

NIH-PA Author Manuscript

NIH-PA Author Manuscript

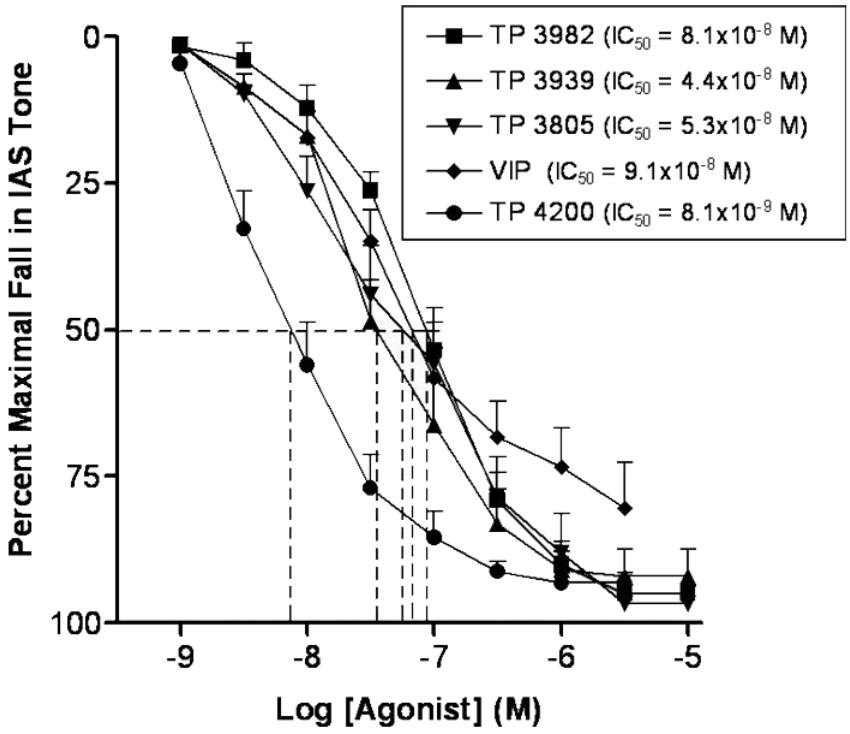

Fig. 2.

Effect of increasing concentration of VIP_{28} and its analogues as % relaxivity of the tissue. IC_{50} values are presented in the inset table

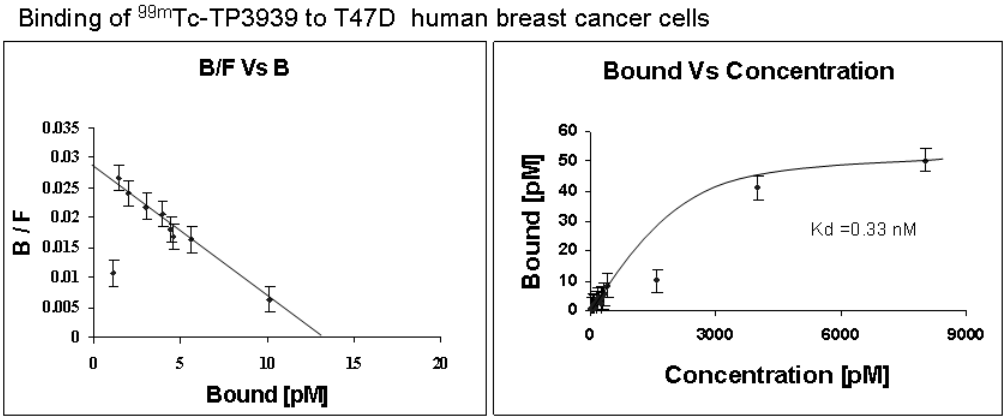

Fig. 3.

The cell binding data plotted as per Scatchard for ^{99m}Tc-TP3939. Binding was performed using T47D human breast cancer cells that express VPAC1 receptors. In this case we used ^{99m}Tc instead of ^{64}Cu, as the biological activity of peptide analogues is not influenced by the tracer used. The saturable plot represents receptor specific binding. The Kd (−1/slope) was estimated using the NIH Chemical Genomics Center, Assay Guidance Manual [Version 4:1; Receptor Binding Assays.htm]. The Kd values as calculated for the other analogues are given in Table. 2.

NIH-PA Author Manuscript NIH-PA Author Manuscript NIH-PA Author Manuscript

NIH-PA Author Manuscript

NIH-PA Author Manuscript

NIH-PA Author Manuscript

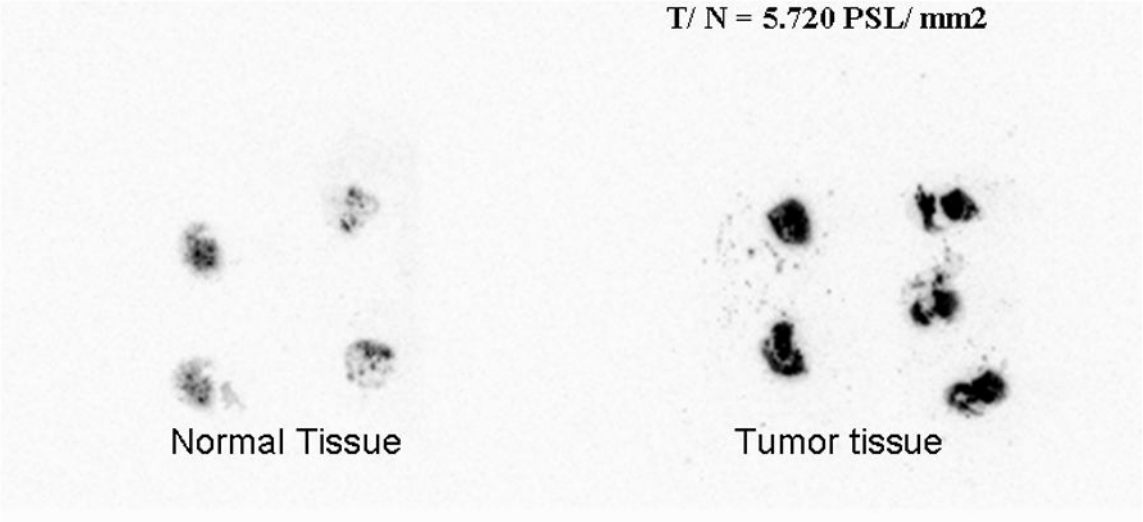

Fig. 4.

Example of digital autoradiography in normal and breast cancer tissues were incubated with ^{64}Cu-TP4200. The images and the calculated tumor and normal PSL/mm^2 invariably reflect higher receptor expression in the tumor tissues. These results were consistent with those of the corresponding RT-PCR analytical data.

NIH-PA Author Manuscript
NIH-PA Author Manuscript
NIH-PA Author Manuscript

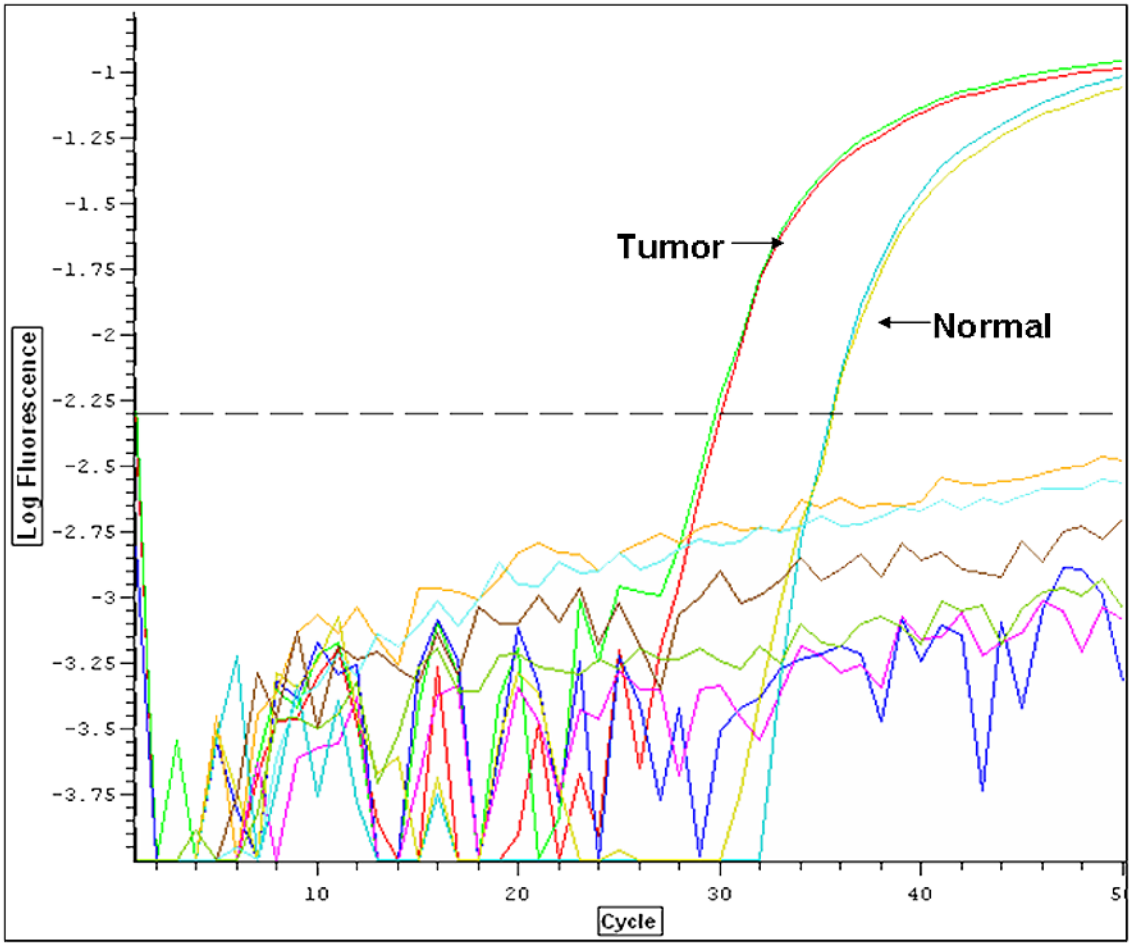

Fig. 5.

RT-PCR of normal and human breast cancer tissues revealing distinct cycle difference between the tumor and the normal tissue. The fewer cycles are required to amplify the protein from tumor tissue as compared to the normal tissue. The density of VPAC1 receptors are more in the tumor tissue (T/N = 5 to 118) than that on the normal breast tissue.

NIH-PA Author Manuscript
NIH-PA Author Manuscript
NIH-PA Author Manuscript

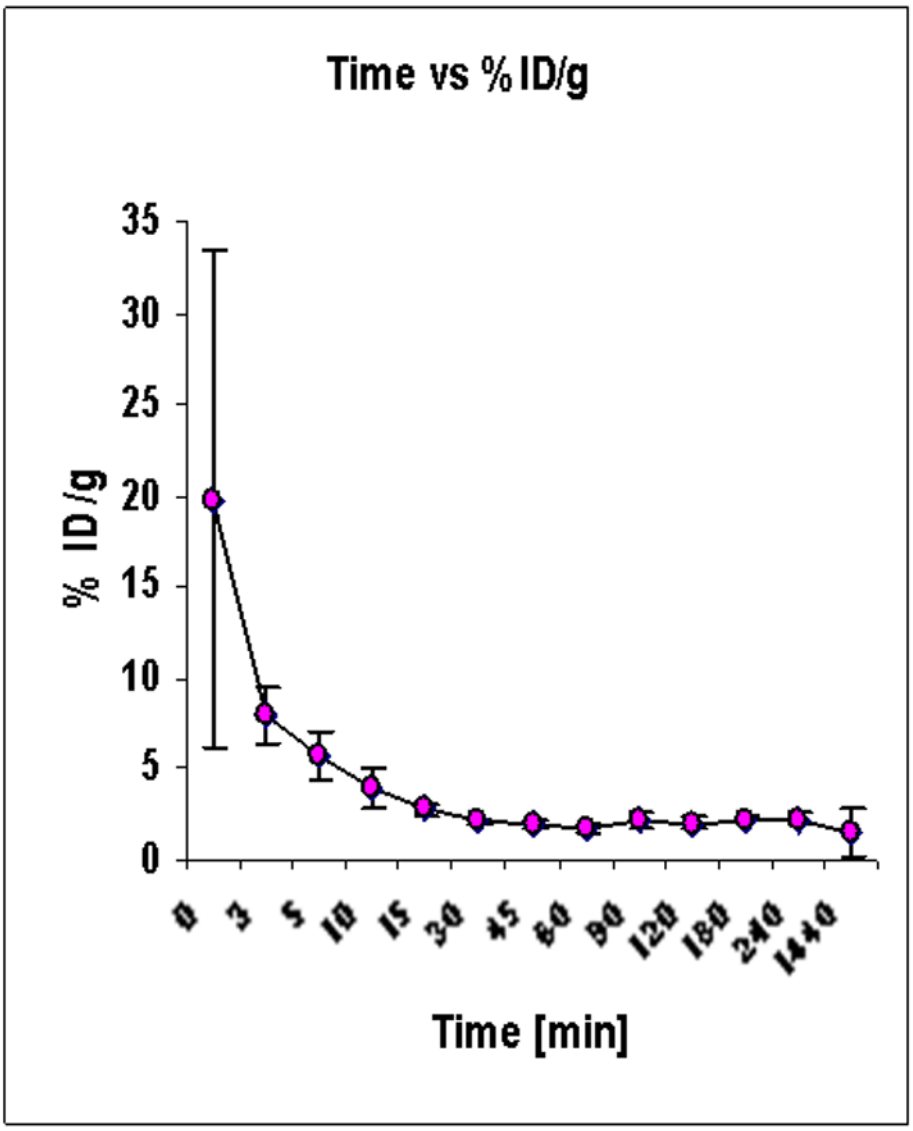

Fig. 6.
The blood clearance study of one of the analogues, TP4200. The clearance curve is biphasic, α t½ = 3.3 min and the β t½ = 150 min.

NIH-PA Author Manuscript

NIH-PA Author Manuscript

NIH-PA Author Manuscript

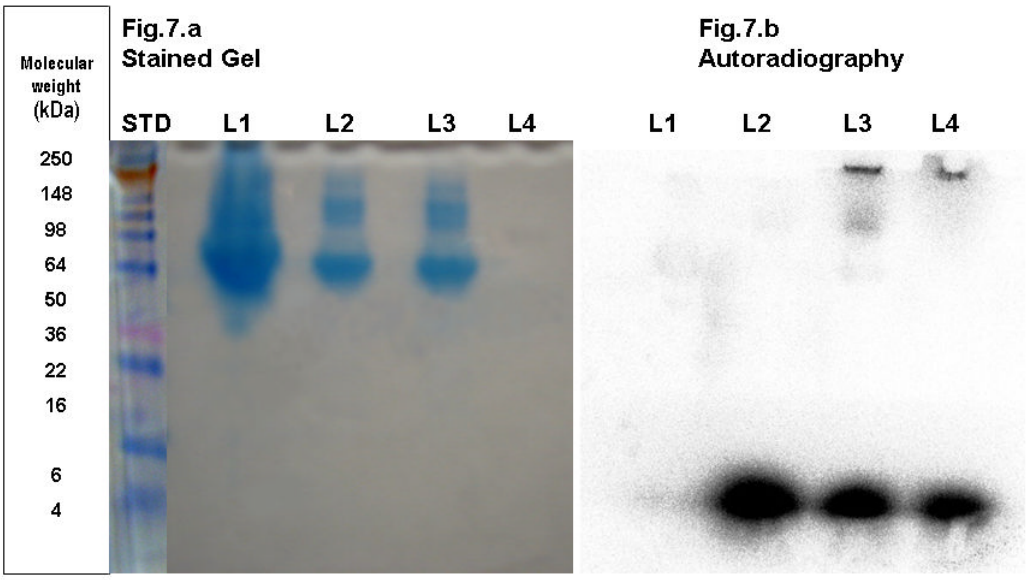

STD: Molecular with standard. **L1**-Lane 1: ^{64}Cu-TP3939 in mouse serum, **L 2-** lane 2: ^{64}Cu-TP3939 with HSA, **L 3** - Lane 3: $^{64}CuCl_2$ with HSA, **L 4-** lane 4: $^{64}CuCl_2$

Fig. 7.

Fig. 7.a. at the left is a Coomassie blue stained gel representing the protein bands and their approximate molecular weight and Fig. 7.b at right is the autoradiography representing ^{64}Cu radioactivity associated with the corresponding proteins. Lane 1: Invivo ^{64}Cu-TP3939 in mouse serum, Lane 2: ^{64}Cu-TP3939 incubated with HSA, exvivo, Lane 3: $^{64}CuCl_2$ incubated with HSA exvivo and Lane 4: $^{64}CuCl_2$.

NIH-PA Author Manuscript

NIH-PA Author Manuscript

NIH-PA Author Manuscript

Table 1

Amino acid sequence, molecular weight and purity of the analogues.

Name of analogue	Observed Molecular weight [amu]	Calculated Molecular weight [amu]	Sequence of amino acids
TP3939	3939.4	3939	His-Ser-Asp-Ala-Val-Phe-Thr-Asp-Asn-Tyr-Thr-Lys-Leu-Arg-Lys-Gln-Nle-Ala-Val-Lys-Lys-(3-OCH3,4-OH) Phe
TP3982	3982.7	3982	His-Ser-Asp-Ala-Val-Phe-Thr-Asp-Asn-Tyr-Thr-Arg-Leu-Arg-Lys-Gln-Met-Ala-Val-Lys-Lys-Tyr-Leu-Asn-Ser-Ile
TP4200	4200.5	4200	Ac-His-Ala-Asp-Ala-Val-Phe-Thr-Glu-Asn-Tyr-Thr-Lys-Leu-Arg-Lys-Gln-Nle-Ala-Ala-Lys-c(-Lys-Tyr-Leu-Asn-
TP3805	3804.5	3805	His-Ser-Asp-Gly-Ile-Phe-Thr-Asp-Ser-Tyr-Ser-Arg-Tyr-Arg-Lys-Gln-Met-Ala-Val-Lys-Lys-Tyr-Leu-Ala-Ala-Val-

NIH-PA Author Manuscript

NIH-PA Author Manuscript

NIH-PA Author Manuscript

Table 2

IC_{50} and Kd values of VIP_{28} and its analogues

Analogue	IC_{50}	Kd
TP3939	4.4×10^{-8}M	0.33×10^{-9}M
TP3982	8.1×10^{-8}M	0.2×10^{-9}M
TP4200	8.1×10^{-9}M	0.72×10^{-9}M
TP3805	5.3×10^{-8}M	3.3×10^{-9}M
VIP_{28} [control]	9.0×10^{-8}M	15×10^{-9}M

NIH-PA Author Manuscript NIH-PA Author Manuscript NIH-PA Author Manuscript

Table 3

Results of human breast cancer tissue autoradiography and RT-PCR (ratios for tumor/normal tissue for each analogue)

HPR	^{64}Cu-TP3939	^{64}Cu-TP3982	^{64}Cu-TP4200	^{64}Cu-TP3805	RT-PCR T/N
Invasive ductal, gr-3 (n= 10)	3.36–10.69	2.83–10.93	3.97–5.13	2.17–9.55	5–118
Insitu micropapillary (n= 1)	2.6	ND	ND	ND	6
Insitu microinvasive- high grade (n= 1)	ND	ND	3.77	2.82	29.78
Tubulolobular (n= 1)	ND	2.94	3.2	ND	ND

ND = Not Done, HPR = Histopathological Report

NIH-PA Author Manuscript

NIH-PA Author Manuscript

NIH-PA Author Manuscript

Table 4

PAGE Analysis. % Radioactivity and estimated molecular weight.

	Lane 1	Lane 2	Lane 3	Lane 4
Molecular Weight (kDa)	**^{64}Cu-TP3939 in serum (Invivo)**	**^{64}Cu-TP3939 with HSA**	**$^{64}CuCl_2$ with HSA**	**$^{64}CuCl_2$**
>98	10.08%	0.47%	2.25%	2.46%
50–64	4.03%	0.25%	0.17%	0.38%
6–16	1.23%	0.09%	0.16%	0.45%
4	25.05%	37.27%	27.27%	22.37%
<4	58.86%	61.92%	70.15%	74.37%